



Adsorption of phenolic compounds from aqueous solution using salicylic acid type adsorbent

Fuqiang An*, Ruikui Du, Xiaohua Wang, Min Wan, Xin Dai, Jianfeng Gao

Department of Chemical, North University of China, Taiyuan 030051, People's Republic of China

ARTICLE INFO

Article history:

Received 13 March 2011

Received in revised form 7 November 2011

Accepted 9 November 2011

Available online 18 November 2011

Keywords:

Poly(glycidyl methacrylate)

5-Aminosalicylic acid

Silica gel

Adsorption

Phenol

ABSTRACT

In this study, 5-aminosalicylic acid (5-ASA) was successfully grafted onto the poly(glycidyl methacrylate) (PGMA) macromolecular chains of PGMA/SiO₂ to obtain adsorbent ASA-PGMA/SiO₂. The adsorption properties of ASA-PGMA/SiO₂ for phenolic compounds were studied through batch and column methods. The experimental results showed that ASA-PGMA/SiO₂ possesses strong adsorption ability for phenolic compounds, and its adsorption capacity for phenol, 4-chlorophenol, and *p*-nitrophenol reaches 1.0, 1.1, and 1.32 mmol g⁻¹, respectively. In addition, pH has a great influence on the adsorption capacity. The adsorption isotherm data obeyed the Langmuir model well than Freundlich model. The desorption of phenolic compounds from the ASA-PGMA/SiO₂ adsorbent was most effectively achieved in a 0.1 mol L⁻¹ sodium hydroxide solution. Consecutive adsorption–desorption experiments showed that the ASA-PGMA/SiO₂ adsorbent could be reused almost without any loss in the adsorption capacity.

© 2011 Elsevier B.V. All rights reserved.

1. Introduction

Phenol and its derivatives are multipurpose raw materials in chemical industry and widely used or generated in many industries such as petroleum, chemicals, petrochemical, coal gasification and carbonization, pharmaceutical, wood, plastic, paper, textile, rubber, photographic, dye, disinfectant and pesticide industries [1,2]. However, they are also main pollutants in surface waters or groundwater. Phenol-contained wastewater can cause protein degradation, tissue erosion and paralysis of the central nervous system and can damage the kidney, liver and pancreas even at very low concentrations due to its high toxicity, poor biodegradability and accumulation in the environment. The Environmental Protection Agency (EPA) has listed phenol and its derivatives on the priority pollutants list. Therefore, it is necessary to remove phenolic pollutants from wastewaters before discharge into water bodies.

Various methods and technologies, such as biodegradation [3–5], photocatalytic degradation [6–8], chemical coagulation [9], chemical oxidation [10,11], solvent extraction [12,13], membrane separation [14,15], and adsorption with porous inorganic materials [16–20] and synthetic polymeric adsorbents [21–24], have been studied and employed to treat the phenol-contained wastewater. Among these methods and technologies, adsorption is still the most attractive and widely used. However, the porous inorganic

materials have some disadvantages, such as lower adsorption capacity, higher operation costs, and lower regenerability and so on. Therefore, functional polymers microspheres or grafted polymers have been increasingly used as adsorbents for efficient treatment of phenol-contained wastewater because of the relatively lower cost, and effective in removing phenolic compounds from wastewaters even at low concentrations.

Among the polymerizable monomers, glycidyl methacrylate (GMA) is a commercial industrial material. Poly(glycidyl methacrylate) (PGMA) has good mechanical strength, sustained acid and base resistance, ease of porosity formation, and high reactivity of the epoxy group. Thus, numerous chelating resins have been successfully prepared via an epoxy group reaction of PGMA with amines except 5-aminosalicylic acid (5-ASA) [25–31]. As regards the chemical structure, 5-ASA possesses one carboxyl, one hydroxyl, and one amine group that can form hydrogen bond interaction with hydroxyl of phenol. Furthermore, 5-ASA can be easily introduced to the side chain of a polymer owing to the reactive amine hydrogen that responds to the epoxy groups.

In this study, the chemical structure of the adsorbent was well designed. First, GMA was grafted onto the silica gel surface to obtain the PGMA/SiO₂ composite material. Then, the adsorbent ASA-PGMA/SiO₂ was obtained through ring-opening reactions between the amine of 5-ASA and the epoxide rings of PGMA. This novel adsorbent ASA-PGMA/SiO₂ possesses not only higher functionality than silica gel, but also higher chemical and mechanical property than PGMA microsphere. The adsorption ability and adsorption kinetic to phenolic compounds were investigated using batch and column methods.

* Corresponding author. Tel.: +86 351 3921414; fax: +86 351 3922118.

E-mail addresses: anfuqiang@nuc.edu.cn, qqfengxiaojin@126.com (F. An).

2. Experimental

2.1. Materials and instruments

Silica was purchased from the Ocean Chemical Company, Ltd. (120–160 mesh, about 125 μm in diameter, pore size: 6 nm, pore volume: 1.0 mL g^{-1} , surface area: 350 $\text{m}^2 \text{g}^{-1}$, Qingdao, China). Glycidyl methacrylate (GMA) was purchased from Ruijinte Chemical Ltd. (Tianjin, China, AR grade and purified by distillation under vacuum. 3-methacryloylpropyl trimethoxysilane (MPS) was purchased from Nanking Chuangshi Chemical Aux Ltd. (Jiangsu, China, AR grade). Azobisisobutyronitrile (AIBN) was purchased from Shanghai Chemical Reagent Plant (Shanghai, China, AR grade). AIBN was recrystallized before use. 5-aminosalicylic acid (5-ASA) and other reagents were purchased from Beijing Chemical Plant (Beijing, China, AR grade). Phenol and other chemicals were purchased from the Beijing Chemical Plant (Beijing, China, AR grade).

Instruments used in this study were as follows: STA449 thermogravimetric analyzer (TGA, Netzsch Company, Germany), Perkin-Elmer1700 infrared spectrometer (Perkin-Elmer Company, American), Unic-2602 UV–vis spectrophotometer (Unic Company, American), PHS-2 acidimeter (The Second Analytical Instrument Factory of Shanghai, China), THZ-92C constant temperature shaker (Boxun Medical Treatment Equipment Factory of Shanghai, China), 438VP scanning electron microscope (LEO Company, England), and NOVA3000 surface area analyzer (Beishide Instrument-S&T. Co., Ltd.).

2.2. Preparation and characterization of adsorbent ASA-PGMA/SiO₂

To prepare the adsorbent ASA-PGMA/SiO₂, 10 g of silica gel particles activated with methane sulfoacid and 15 mL of coupling agent MPS were added into 200 mL of a mixed solvent of ethanol and water (V/V = 1:1). The contents were maintained for 24 h at 50 °C, resulting in the formation of the surface-modified particles MPS-SiO₂, on which polymerizable double bonds were attached chemically. Afterwards, 6 g of particles MPS-SiO₂ and 20 mL of GMA were added into 400 mL of dimethyl formamide (DMF). Graft polymerization was performed by initiating of AIBN (1.4 wt% of monomer) under N₂ atmosphere at 70 °C for 24 h. The product particles were extracted with acetone in a Soxhlet apparatus to remove the polymers attaching physically onto the particles and then dried under vacuum, and finally the composite material PGMA/SiO₂ were gained. Subsequently, 1 g of PGMA/SiO₂ and 6 g of 5-ASA were added into 100 ml of sodium hydroxide aqueous solution with pH of 12. The ring-opening reaction between the amine of 5-ASA and the epoxide ring of PGMA was allowed to take place at 80 °C for 24 h, and finally, the adsorbent ASA-PGMA/SiO₂ was obtained. The preparation process of ASA-PGMA/SiO₂ is expressed in Scheme 1. The grafting degree of ASA-PGMA/SiO₂ was determined by the TGA method and surface area was determined by the NOVA3000 surface area analyzer. The ASA-PGMA/SiO₂ used in this study have a grafting degree of 0.168 g g^{-1} and surface area of 342 $\text{m}^2 \text{g}^{-1}$.

2.3. Batch adsorption

2.3.1. Measurement of kinetic adsorption curve

About 0.01 g of ASA-PGMA/SiO₂ and 25 ml of aqueous metal ion solution with an initial concentration (C_0) of 1 mmol L^{-1} (pH of 6) were directly introduced into a conical flask. This conical flask was placed into a shaker at a presettled temperature and then shaken. At different time, the concentration (C_t) of phenol solution was determined by UV analysis performed on a UV–vis spectrophotometer with the wavelength at 270 nm (*p*-nitrophenol at 314 nm,

4-chlorophenol at 228 nm). The adsorption capacity (Q) was calculated according to the following equation.

$$Q = \frac{V(C_0 - C_t)}{m} \quad (1)$$

where Q (mmol g^{-1}) is the adsorption capacity; V (L) is the volume of the solution; m (g) is the weight of the adsorbent ASA-PGMA/SiO₂.

2.3.2. Measurement of adsorption isotherm

About 0.01 g of ASA-PGMA/SiO₂ and 25 ml aqueous solution of metal ion with different initial concentrations ($C_0 = 0.2, 0.4, 0.6, 0.8$ and 1 mmol L^{-1}) and the same pH of 6 were directly introduced into several conical flasks. These conical flasks were placed into a shaker at a presettled temperature and then shaken. After reaching the adsorption equilibrium (10 h), the equilibrium concentration (C_e) was determined by UV analysis performed on a UV–vis spectrophotometer. The equilibrium adsorption capacity (Q_e) was calculated according to the following equation.

$$Q_e = \frac{V(C_0 - C_e)}{m} \quad (2)$$

2.4. Column adsorption and elution experiment

In the column experiment, 1.2514 g of ASA-PGMA/SiO₂ was placed in a glass column 8 mm in diameter and with a bed volume (BV) of 2 ml. The phenol solution with concentration of 1 mmol L^{-1} and pH of 6 was allowed to flow gradually through the column at a rate of five bed volumes per hour (5 BV h⁻¹). The effluent with one bed volume was collected, the concentration of phenol was determined, and the dynamics adsorption curve was measured. The leaking adsorption capacity and the saturated adsorption capacity were also calculated.

The elution experiment was performed using sodium hydroxide solution with a concentration of 0.01 mol L^{-1} as eluting agent. The flow rate of the eluting agent was controlled at 1 BV h⁻¹. The eluent with one bed volume was collected, the concentration was determined, and the elution curve was plotted.

2.5. Repeated use experiment

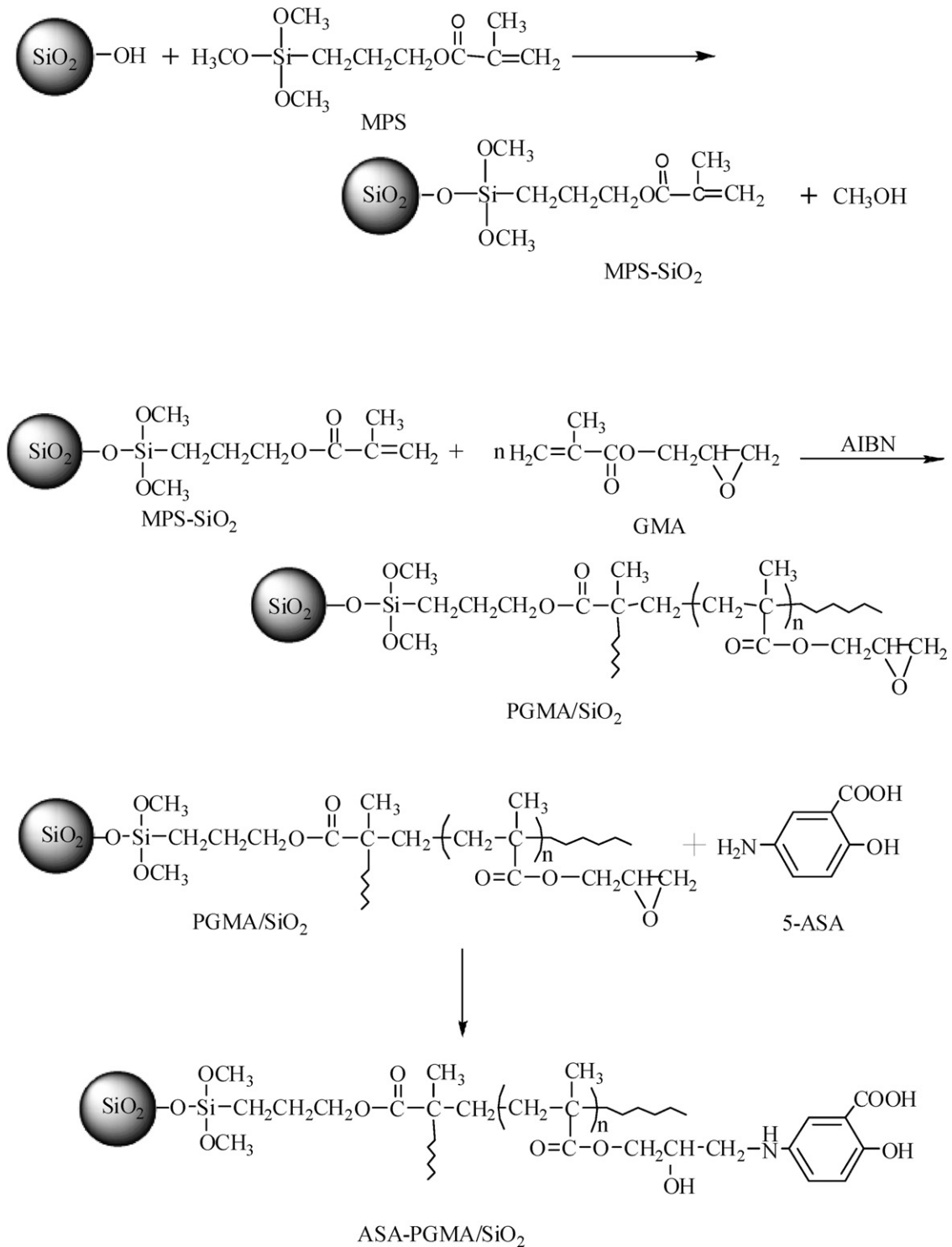
Repeated usability (i.e., regenerability) is an important factor for an effective adsorbent. Desorption of the adsorbed phenol from ASA-PGMA/SiO₂ was also studied by batch experiment using 0.1 mol L^{-1} of sodium hydroxide solution as eluent. The ASA-PGMA/SiO₂ adsorbed phenol was placed in the eluent and stirred continuously at room temperature (20 °C) for 5 h. The final concentration of aqueous phase was determined. Desorption ratio was calculated from the capacity and final concentration in the eluent. In order to test the reusability of ASA-PGMA/SiO₂, adsorption–desorption procedure was repeated 10 times using the same ASA-PGMA/SiO₂.

3. Results and discussion

3.1. Preparation and characterization of adsorbent ASA-PGMA/SiO₂

To confirm the effectiveness of PGMA grafting onto the silica gel and 5-ASA grafting onto the PGMA/SiO₂, the FTIR spectra of the SiO₂, MPS-SiO₂, PGMA/SiO₂ and ASA-PGMA/SiO₂ were obtained through FTIR spectrometers and shown in Fig. 1.

In the infrared spectrum of PGMA/SiO₂, the characteristics absorptions of epoxide rings appear at 905 cm^{-1} , and the characteristics absorptions of carbonyl group at 1732 cm^{-1} was enhanced.



Scheme 1. Synthesis process of adsorbent ASA-PGMA/SiO₂.

These show that PGMA macromolecules have been grafted onto the silica gel surface, and PGMA/SiO₂ has been formed.

The characteristics absorptions of benzene ring appear at 1485 cm⁻¹ and 1589 cm⁻¹, respectively, the characteristics absorptions of bend vibration of C–N bond appear at 1408 cm⁻¹, the characteristics absorptions of epoxide rings at 905 cm⁻¹ was disappeared, and the characteristics absorptions of N–H bond at 3492 cm⁻¹ was enhanced. These show that 5-ASA has been reacted with PGMA of PGMA/SiO₂, and ASA-PGMA/SiO₂ has been formed.

Fig. 2 is the SEM of SiO₂ and ASA-PGMA/SiO₂. It can be seen that the surface of ASA-PGMA/SiO₂ is smoother than that of SiO₂. This implied that the macromolecular was grafted onto the silica gel surface.

3.2. Kinetic adsorption curve

The kinetic adsorption curve is shown in Fig. 3. The adsorption reached to equilibrium at 10 h, and the saturated adsorption

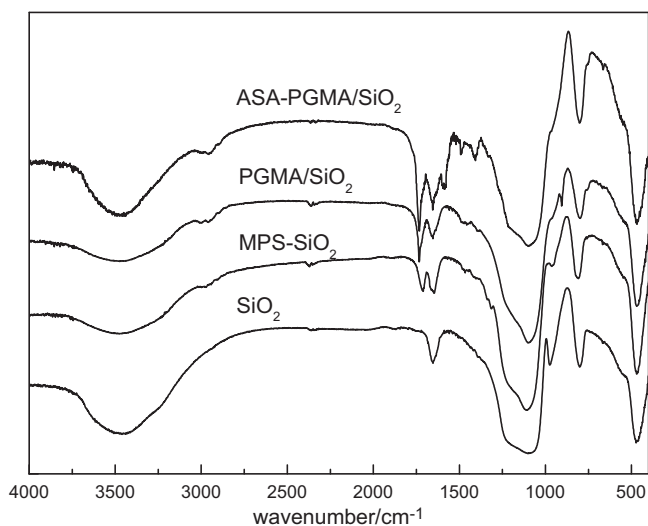


Fig. 1. FTIR spectra of every microgranules.

capacity for phenol, 4-chlorophenol and *p*-nitrophenol reached 1.0, 1.1, and 1.32 mmol g⁻¹, respectively. The adsorption capacity (94 mg g⁻¹) of ASA-PGMA/SiO₂ for phenol is higher than that of other adsorbents, such as zeolite (0.25 mg g⁻¹) [16], Hap nanopowders (0.2–10.3 mg g⁻¹) [19], and tirebolu bentonite (8 mg g⁻¹) [20]. The adsorbent ASA-PGMA/SiO₂ clearly has very strong adsorption ability and high affinity for phenolic compounds. This can be attributed mainly to the hydrogen bond interaction between the 5-ASA on ASA-PGMA/SiO₂ and phenolic compound, and the interaction mechanism will be discussed below. In addition, the adsorption capacity for 4-chlorophenol and *p*-nitrophenol is higher than phenol; this is due to the -Cl and -NO₂ as acceptor of hydrogen bond in 4-chlorophenol and *p*-nitrophenol molecule.

Additional, the surface area of ASA-PGMA/SiO₂ (342 m² g⁻¹) is accordant to that of PGMA/SiO₂ (350 m² g⁻¹). This indicated again that the main adsorption force is not the higher surface area but the hydrogen bond interaction.

3.3. Adsorption isotherm

The adsorption isotherms of ASA-PGMA/SiO₂ for phenol, 4-chlorophenol and *p*-nitrophenol are shown in Fig. 4. It can be seen that the equilibrium adsorption capacity increases rapidly with the increase of the equilibrium concentrations. This also implied that

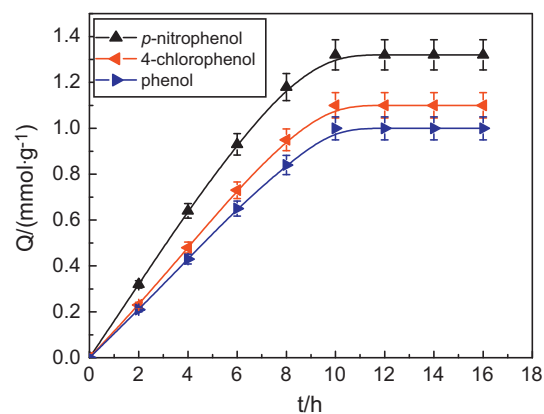


Fig. 3. Kinetic adsorption curve of ASA-PGMA/SiO₂ for phenolic compounds Temperature: 20 °C; pH=6.

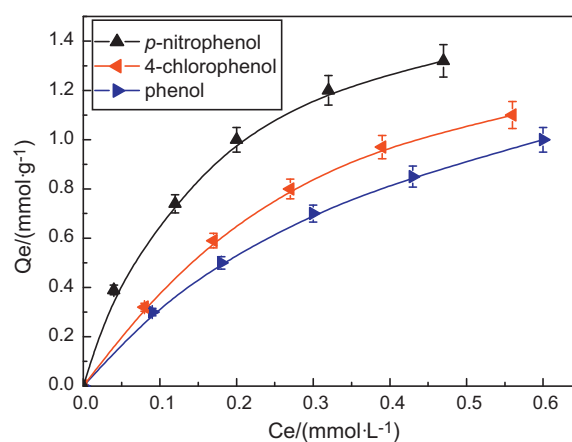


Fig. 4. Adsorption isotherms of ASA-PGMA/SiO₂ for phenolic compounds Temperature: 20 °C; Adsorption time: 10 h; pH=6.

ASA-PGMA/SiO₂ possesses very strong adsorption ability and high affinity for phenolic compounds.

Freundlich adsorption equation and its logarithms form are follows:

$$Q_e = k C_e^{1/n} \quad (3)$$

$$\ln Q_e = \ln k + \frac{1}{n} \ln C_e \quad (4)$$

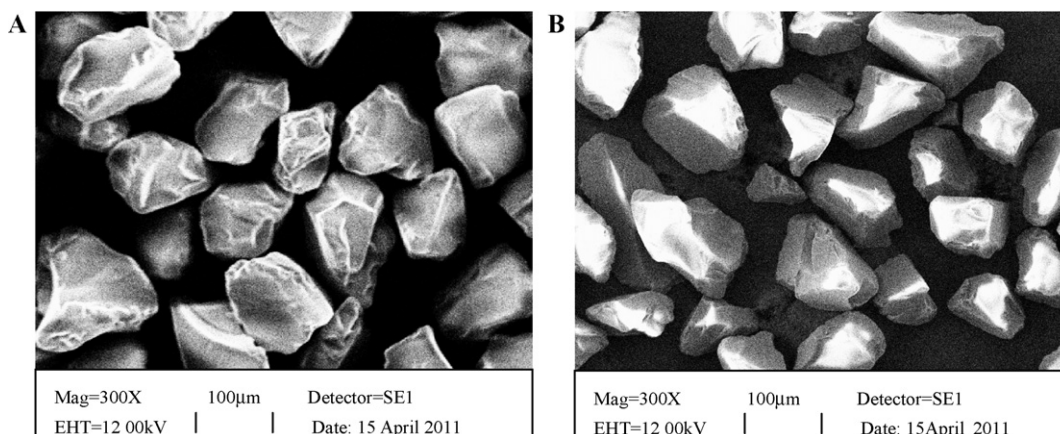


Fig. 2. SEM of SiO₂(A) and ASA-PGMA/SiO₂ (B).

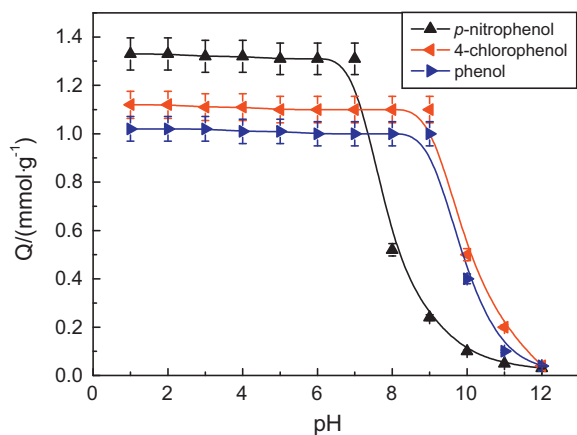


Fig. 5. The influence of pH on the adsorption capacity. Temperature, 20 °C; adsorption time, 10 h.

Langmuir adsorption equation is as follows:

$$Q_e = Q_m \frac{bC_e}{1 + bC_e} \quad (5)$$

$$\frac{C_e}{Q_e} = \frac{C_e}{Q_m} + \frac{1}{bQ_m} \quad (6)$$

where Q_m (mmol g^{-1}) is the saturated adsorption capacity; b is the combine constant.

The data in Fig. 3 are treated using Freundlich adsorption equation and Langmuir adsorption equation, and the related constant and linear regression coefficient is displayed in Table 1.

It can be seen that the combine constant (b and k) of Langmuir adsorption equation and Freundlich adsorption equation is increase in the sequence of phenol, 4-chlorophenol, p -nitrophenol, and this order is in accord with the order of adsorption capacity. The linear regression coefficient is very close to 1. This indicated that the adsorption of ASA-PGMA/SiO₂ for phenolic compounds is a typical monomolecular adsorption.

3.4. The influence of pH value on adsorption capacity

Fig. 5 shows the adsorption performances of ASA-PGMA/SiO₂ for phenol, 4-chlorophenol and p -nitrophenol at different solution pH values.

Obviously, the pH has a great influence on the adsorption capacity of ASA-PGMA/SiO₂ for phenolic compounds. With increasing pH value, the adsorption capacity of ASA-PGMA/SiO₂ for phenol does not change obviously at first, but decreases sharply after pH 9. The same trend appeared for 4-chlorophenol and p -nitrophenol, but the turning point is pH 9 and 7, respectively. The turning point is relevant with its pK_a value.

There are hydrogen bond interaction and π - π stacking interaction between ASA and phenols. As pH value is lower, there are lots of hydrogen ions H^+ in solution, and the carboxyl groups and hydroxyl groups do not dissociate. Under the driving of π - π stacking interaction, hydrogen bond could be formed easily. So the adsorption ability is the strongest and the adsorption capacity is the highest. The dissociation degree of the carboxyl groups and hydroxyl groups is enhanced with the increases of pH value, resulting in weakening and decrease of hydrogen bond. So the adsorption capacity decline with the increase of pH value. When of solution goes beyond the pK_a of phenols, hydroxyl groups of phenol were neutralized and phenols chiefly exist as negative phenolate ions. Therefore, hydrogen bond could not be formed although the weak π - π stacking interaction still exists. So adsorption capacity is very low.

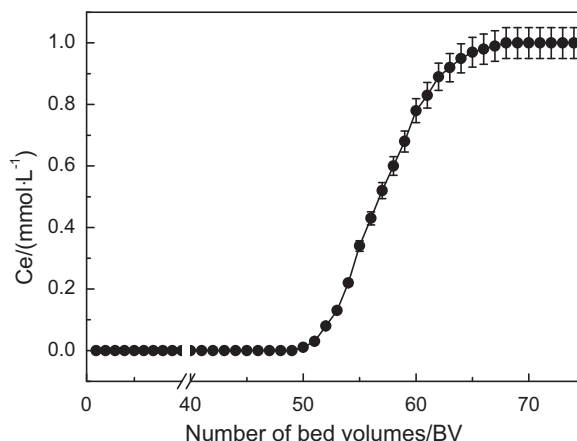


Fig. 6. Breakthrough curve of phenol on ASA-PGMA/SiO₂ column. Temperature, 20 °C; pH = 6.

The low adsorption capacity at high pH value indicates that the spent adsorbent can be regenerated in strong basic solution.

3.5. Dynamic adsorption curve

Fig. 6 shows the dynamic adsorption curve of ASA-PGMA/SiO₂ for phenol. It can be found that when solution passes through the column packed with ASA-PGMA/SiO₂ at a flow rate of 5 bed volumes per hour (5 BV h^{-1}) upstream, the leaking appears at 50 BV, the leaking adsorption capacity to be calculated is 0.78 mmol g^{-1} , and the saturated adsorption capacity is 0.99 mmol g^{-1} that analogous to the static adsorption result.

3.6. Elution curve

Good desorption performance of an adsorbent is important in its potential practical applications. From the results in Fig. 4, it has been found that the ASA-PGMA/SiO₂ did not adsorb phenols as $\text{pH} > 12$, suggesting that the adsorbed phenols on the ASA-PGMA/SiO₂ may be desorbed in strong basic solution with a pH value of 12. Sodium hydroxide solution with a concentration of 0.01 mol L^{-1} is used as the eluent, and the eluent at a rate of 1 BV h^{-1} flows upstream through the column of ASA-PGMA/SiO₂ on which the adsorption of phenol has reached to saturation. The elution curve of ASA-PGMA/SiO₂ is shown in Fig. 7, and desorption ratio was calculated as follow:

$$\text{Desorption ratio} = \frac{\text{amount of phenol desorbed to the elution medium}}{\text{amount of phenol sorbed on adsorbent}} \times 100\% \quad (7)$$

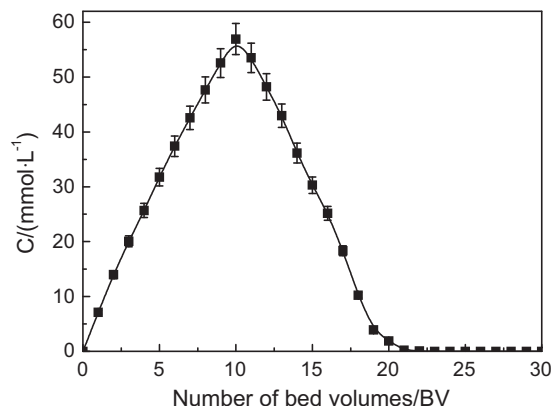


Fig. 7. Elution curve of ASA-PGMA/SiO₂. Temperature, 20 °C.

Table 1
The related constant and linear regression coefficient of Langmuir–Freundlich fitting.

Fitting model	Parameter	Uncertainty	Adsorbate		
			Phenol	4-Chlorophenol	<i>p</i> -Nitrophenol
Langmuir	<i>b</i>	±0.5%	2.76	3.40	7.23
	<i>R</i> ²		0.9924	0.9973	0.9986
Freundlich	<i>k</i>	±0.5%	2.08	1.70	1.51
	<i>n</i>	±0.5%	1.59	1.66	2.00
	<i>R</i> ²		0.9811	0.9799	0.9768

It can be seen that the shape of desorption curve is cusplate and without tailing, and it shows fine elution result. The calculation results show that within 18 and 22 bed volumes, phenol is eluted from ASA-PGMA/SiO₂ column with a desorption ratio of 95.29% and 97.93%, respectively. The fact reveals fully that ASA-PGMA/SiO₂ has outstanding elution property, and this novel adsorbent ASA-PGMA/SiO₂ has excellent reusing property.

3.7. Reusability

In order to show the reusability of ASA-PGMA/SiO₂, adsorption-desorption cycle was repeated 10 times by using the same material.

Adsorption-desorption cycle of ASA-PGMA/SiO₂ is shown in Fig. 8. The results clearly showed that the ASA-PGMA/SiO₂ could be used repeatedly without significantly losing its adsorption amount.

3.8. Real sample analysis

To demonstrate its potentially application value, the adsorbent ASA-PGMA/SiO₂ was used to dispose there kinds of wastewater by batch method, such as wastewater containing phenol (10.5 mmol L⁻¹) and formaldehyde (11.2 mmol L⁻¹) from bakelite plant, wastewater containing 4-chlorophenol (5.22 mmol L⁻¹) and phosazetim (3.14 mmol L⁻¹) from pesticide plant, and wastewater containing *p*-nitrophenol (2.84 mmol L⁻¹) and phenacetinum (1.06 mmol L⁻¹) from pharmaceutical factory.

In the batch study, 200 mL of wastewater was disposed using the adsorbent ASA-PGMA/SiO₂. The removal rate (*R*) was calculated according to the following equation and shown in Figs. 9–11.

$$R = \frac{C_0 - C_e}{C_0} \quad (8)$$

For 200 mL of wastewater containing phenol and formaldehyde, the removal rate of ASA-PGMA/SiO₂ for phenol could reach 98.0%

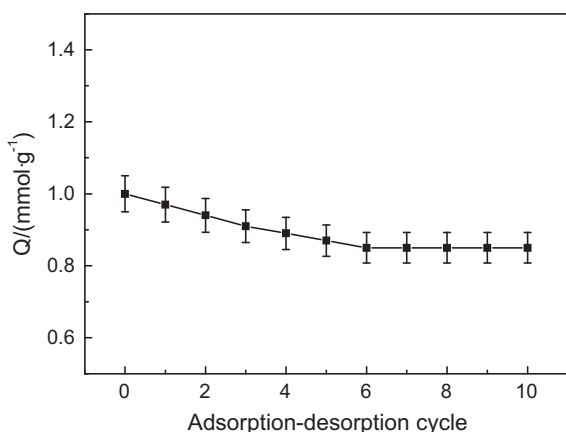


Fig. 8. Adsorption-desorption cycle of ASA-PGMA/SiO₂.

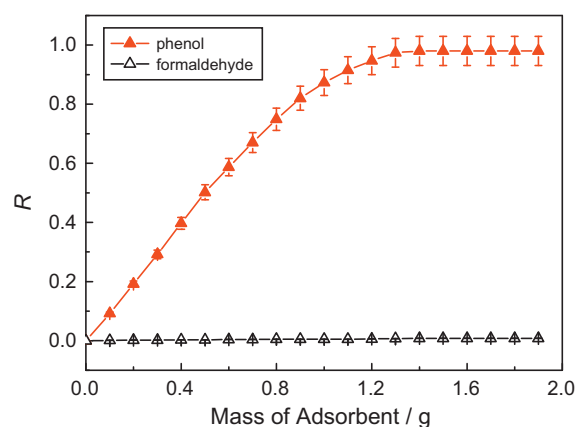


Fig. 9. The removal rate curve for phenol and formaldehyde.

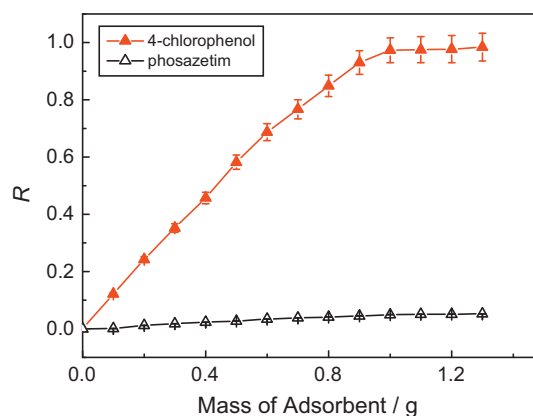


Fig. 10. The removal rate curve for 4-chlorophenol and phosazetim.

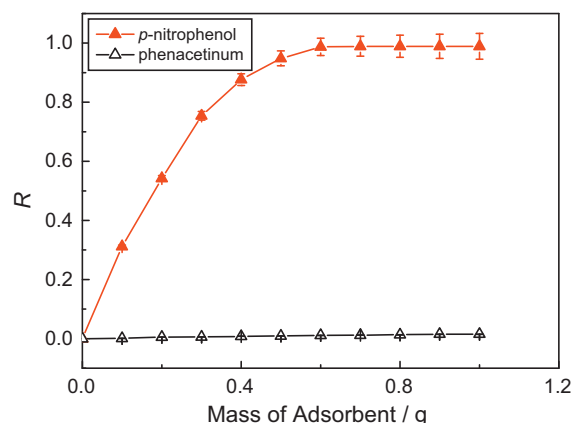


Fig. 11. The removal rate curve for *p*-nitrophenol and phenacetinum.

Table 2
Distribution coefficient and selectivity coefficient data of ASA-PGMA/SiO₂.

$K_d(\text{Lg}^{-1})$		k	$K_d(\text{Lg}^{-1})$		k	$K_d(\text{Lg}^{-1})$		k
Phenol	Formaldehyde		4-Chlorophenol	Phosazetim		<i>p</i> -Nitrophenol	phenacetinum	
1.24	0.06	20.67	3.84	0.26	14.77	4.62	0.11	42.00

when 1.4 g of ASA-PGMA/SiO₂ was used, while the removal rate for formaldehyde is very low ($R < 0.9\%$).

For 200 mL of wastewater containing 4-chlorophenol and phosazetim, the removal rate of ASA-PGMA/SiO₂ for 4-chlorophenol could reach 97.3% when 1.0 g of ASA-PGMA/SiO₂ was used, while the removal rate for phosazetim is very low ($R < 5\%$).

For 200 mL of wastewater containing *p*-nitrophenol and phenacetinum, the removal rate of ASA-PGMA/SiO₂ for *p*-nitrophenol could reach 98.7% when 0.6 g of ASA-PGMA/SiO₂ was used, while the removal rate for phenacetinum is very low ($R < 2\%$).

This result clearly shows that ASA-PGMA/SiO₂ could adsorb selectively phenol, 4-chlorophenol and *p*-nitrophenol from wastewater, and possesses potential application value.

The adsorption capacity towards phenol, 4-chlorophenol and *p*-nitrophenol is very high, but the adsorption capacity towards another competitor species is very low. This indicated that the ASA-PGMA/SiO₂ has excellent selectivity.

In order to show further the selectivity of ASA-PGMA/SiO₂ for every target molecular, distribution coefficients (K_d) were calculated by Eq. (9) [32].

$$K_d = \frac{Q_e}{C_e} \quad (9)$$

The selectivity coefficient (k) of ASA-PGMA/SiO₂ for every target molecular (A) with respect to the competitor species (B) can be obtained according to Eq. (10),

$$k = \frac{K_d(A)}{K_d(B)} \quad (10)$$

Table 2 summarizes the data of the distribution coefficients K_d and selectivity coefficients k .

It could be seen that the distribution coefficient towards target molecular is larger than that towards competitor species, and the selectivity coefficient (k) is very large. This indicated again that ASA-PGMA/SiO₂ has excellent selectivity.

4. Conclusions

In this study, macromolecule poly(glycidyl methacrylate) was grafted onto micron-sized silica gel to prepare the PGMA/SiO₂. And then the novel adsorbent ASA-PGMA/SiO₂ was successfully obtained through ring-opening reactions between amine of 5-ASA and epoxide rings of poly(glycidyl methacrylate). ASA-PGMA/SiO₂ has very strong adsorption ability for phenols. The adsorption ability of ASA-PGMA/SiO₂ for phenols is largely dependent on pH value of solution. This study shows that ASA-PGMA/SiO₂ could dispose wastewater containing phenols. Additional, ASA-PGMA/SiO₂ has excellent reusability and high selectivity.

Acknowledgements

The authors are grateful to the Science Foundation of Province Shanxi of China and National Science Foundation of China for the financial support of this work.

References

- [1] S.H. Lin, R.S. Juang, Adsorption of phenol and its derivatives from water using synthetic resins and low-cost natural adsorbents: a review, *J. Environ. Manag.* 90 (2009) 1336–1349.
- [2] G. Busca, S. Berardinelli, C. Resini, L. Arrighi, Technologies for the removal of phenol from fluid streams: a short review of recent developments, *J. Hazard. Mater.* 160 (2008) 265–288.
- [3] L. Stehlickova, M. Svab, L. Wimmerova, J. Kozler, Intensification of phenol biodegradation by humic substances, *Int. Biodeter. Biodegr.* 63 (2009) 923–927.
- [4] M.H. El-Naas, S. Al-Zuhair, S. Makhlof, Continuous biodegradation of phenol in a spouted bed bioreactor (SBBR), *Chem. Eng. J.* 160 (2010) 565–570.
- [5] E. Kurzbaum, F. Kirzhner, S. Sela, Y. Zimmels, R. Armon, Efficiency of phenol biodegradation by planktonic *Pseudomonas pseudoalcaligenes* (a constructed wetland isolate) vs. root and gravel biofilm, *Water Res.* 44 (2010) 5021–5031.
- [6] R.X. Mu, Z.Y. Xu, L.Y. Li, Y. Shao, H.Q. Wan, S.R. Zheng, On the photocatalytic properties of elongated TiO₂ nanoparticles for phenol degradation and Cr(VI) reduction, *J. Hazard. Mater.* 176 (2010) 495–502.
- [7] P.A. Deshpande, G. Madras, Photocatalytic degradation of phenol by base metal-substituted orthovanadates, *Chem. Eng. J.* 161 (2010) 136–145.
- [8] S. Ahmed, M.G. Rasul, W.N. Martens, R. Brown, M.A. Hashib, Heterogeneous photocatalytic degradation of phenols in wastewater: a review on current status and developments, *Desalination* 261 (2010) 3–18.
- [9] J.A. Perdigon-Melón, J.B. Carbajo, A.L. Petre, R. Rosal, E. García-Calvo, Coagulation-Fenton coupled treatment for ecotoxicity reduction in highly polluted industrial wastewater, *J. Hazard. Mater.* 181 (2010) 127–132.
- [10] V.K. Bansal, P.P. Thankachan, R. Prasad, Catalytic and electrocatalytic wet oxidation of phenol using two new nickel(II) tetraazamacrocyclic complexes under heterogeneous conditions, *J. Mol. Catal. A: Chem.* 316 (2010) 131–138.
- [11] J.A. Zazo, J.A. Casas, A.F. Mohedano, J.J. Rodriguez, Semicontinuous Fenton oxidation of phenol in aqueous solution. A kinetic study, *Water Res.* 43 (2009) 4063–4069.
- [12] N. Messikh, M.H. Samar, L. Messikh, Neural network analysis of liquid-liquid extraction of phenol from wastewater using TBP solvent, *Desalination* 208 (2007) 42–48.
- [13] T. Vatai, M. Škerget, Ž. Knez, Extraction of phenolic compounds from elder berry and different grape marc varieties using organic solvents and/or supercritical carbon dioxide, *J. Food Eng.* 90 (2009) 246–254.
- [14] A. Bódalo, E. Gómez, A.M. Hidalgo, M. Gómez, M.D. Murcia, I. López, Nanofiltration membranes to reduce phenol concentration in wastewater, *Desalination* 245 (2009) 680–686.
- [15] Y.S. Ng, N.S. Jayakumar, M.A. Hashim, Performance evaluation of organic emulsion liquid membrane on phenol removal, *J. Hazard. Mater.* 184 (2010) 255–260.
- [16] M. Sprynskyy, T. Ligor, M. Lebedynets, B. Buszewski, Kinetic and equilibrium studies of phenol adsorption by natural and modified forms of the clinoptilolite, *J. Hazard. Mater.* 169 (2009) 847–854.
- [17] J. Su, H.F. Lin, Q.P. Wang, Z.M. Xie, Z.L. Chen, Adsorption of phenol from aqueous solutions by organomontmorillonite, *Desalination* 269 (2011) 163–169.
- [18] Q.S. Liu, T. Zheng, P. Wang, J.P. Jiang, N. Li, Adsorption isotherm, kinetic and mechanism studies of some substituted phenols on activated carbon fibers, *Chem. Eng. J.* 157 (2010) 348–356.
- [19] K.L. Lin, J.Y. Pan, Y.W. Chen, R.M. Cheng, X.C. Xu, Study the adsorption of phenol from aqueous solution on hydroxyapatite nanopowders, *J. Hazard. Mater.* 161 (2009) 231–240.
- [20] H.B. Senturk, D. Ozdes, A. Gundogdu, C. Duran, M. Soylak, Removal of phenol from aqueous solutions by adsorption onto organomodified Tirebolu bentonite: equilibrium, kinetic and thermodynamic study, *J. Hazard. Mater.* 172 (2009) 353–362.
- [21] F.Q. An, B.J. Gao, X.Q. Feng, Adsorption mechanism and property of novel composite material PMAA/SiO₂ towards phenol, *Chem. Eng. J.* 153 (2009) 108–113.
- [22] X.W. Zeng, Y.G. Fan, G.L. Wu, C.H. Wang, R.F. Shi, Enhanced adsorption of phenol from water by a novel polar post-crosslinked polymeric adsorbent, *J. Hazard. Mater.* 169 (2009) 1022–1028.
- [23] X.W. Zeng, T.J. Yu, P. Wang, R.H. Yuan, Q. Wen, Y.G. Fan, C.H. Wang, R.F. Shi, Preparation and characterization of polar polymeric adsorbents with high surface area for the removal of phenol from water, *J. Hazard. Mater.* 177 (2010) 773–780.
- [24] M. Sobiesiak, B. Podkościelna, Preparation and characterization of porous DVB copolymers and their applicability for adsorption (solid-phase extraction) of phenol compounds, *Appl. Surf. Sci.* 257 (2010) 1222–1227.
- [25] C. Liu, R. Bai, L. Hong, T. Liu, Functionalization of adsorbent with different aliphatic polyamines for heavy metal ion removal: characteristics and performance, *J. Colloid Interface Sci.* 345 (2010) 454–460.

- [26] L. Chen, C. Guo, Y. Guan, H. Liu, Isolation of lactoferrin from acid whey by magnetic affinity separation, *Sep. Purif. Technol.* 56 (2007) 168–174.
- [27] L. Li, F. Liu, X. Jing, P. Ling, A. Li, Displacement mechanism of binary competitive adsorption for aqueous divalent metal ions onto a novel IDA-chelating resin: isotherm and kinetic modeling, *Water Res.* 45 (2011) 1177–1188.
- [28] X. Dong, Y. Zheng, Y. Huang, X. Chen, X. Jing, Synthesis and characterization of multifunctional poly(glycidyl methacrylate) microspheres and their use in cell separation, *Anal. Biochem.* 405 (2010) 207–212.
- [29] S.M. Chergui, N. Abbas, T. Matrab, M. Turmine, E.B. Nguyen, R. Losno, J. Pinson, M.M. Chehimi, Uptake of copper ions by carbon fiber/polymer hybrids prepared by tandem diazonium salt chemistry and in situ atom transfer radical polymerization, *Carbon* 48 (2010) 2106–2111.
- [30] L. Lei, X. Liu, Y. Li, Y. Cui, Y. Yang, G. Qin, Study on synthesis of poly(GMA)-grafted $\text{Fe}_3\text{O}_4/\text{SiO}_x$ magnetic nanoparticles using atom transfer radical polymerization and their application for lipase immobilization, *Mater. Chem. Phys.* 125 (2011) 866–871.
- [31] N. Bereli, G. Şener, E.B. Altıntaş, H. Yavuz, A. Denizli, Poly(glycidyl methacrylate) beads embedded cryogels for pseudo-specific affinity depletion of albumin and immunoglobulin G, *Mater. Sci. Eng. C* 30 (2010) 323–329.
- [32] A. Ersöz, R. Say, A. Denizli, Ni(II) ion-imprinted solid-phase extraction and pre-concentration in aqueous solutions by packed-bed columns, *Anal. Chim. Acta* 502 (2004) 91–97.